



The effect of fabric mass per unit area and blood impact velocity on bloodstain morphology

L. Dicken^a, C. Knock^{a,*}, D.J. Carr^{a,1}, S. Beckett^b

^aCentre for Defence Engineering, Cranfield University at the Defence Academy of the United Kingdom, Shrivenham, SN6 8LA, United Kingdom

^bCranfield Forensic Institute, Cranfield University at the Defence Academy of the United Kingdom, Shrivenham, SN6 8LA, United Kingdom

ARTICLE INFO

Article history:

Received 25 July 2018

Received in revised form 1 May 2019

Accepted 2 May 2019

Available online 9 May 2019

Keywords:

Bloodstain analysis

Absorbent surfaces

Yarn linear density

Micro-computed tomography

Scanning electron microscopy

Wicking

ABSTRACT

This paper discusses the effects of thickness, mass per unit area, sett, yarn linear density and twist of calico fabrics (100% cotton, plain woven) on the morphology of passive bloodstains. Horse blood was dropped vertically onto three calico fabrics with different mass per unit areas (85.1 g/m^2 , 163.5 g/m^2 and 224.6 g/m^2). Six different impact velocities were used (1.7 ms^{-1} , 2.9 ms^{-1} , 4.1 ms^{-1} , 4.9 ms^{-1} , 5.1 ms^{-1} and 5.4 ms^{-1}). The dry bloodstains were largest on the calico with the lightest mass per unit area. The low yarn linear density and large inter-yarn spaces meant that the blood could wick into the yarns from all directions and along the intra-yarn spaces. The calico with the middle mass per unit area had the smallest mean dry bloodstain area for four out of the six velocities. The twist level for this calico was greater than for the calicos with a heavier or lighter mass per unit area. This reduced the amount of wicking which occurred along the yarns due to the tighter yarn structure. The calico with the heaviest mass per unit area had the highest yarn linear density resulting in a thicker fabric, so the blood could not as easily penetrate into the fabric. This resulted in a thicker wet blood layer remaining on the fabric surface, where it gradually wicked vertically into the yarns under gravity. Less wicking along the yarns occurred, resulting in a smaller bloodstain than on the fabric with the lightest mass per unit area. The correlation between impact velocity and mean dry bloodstain area was greater for the calicos with the medium and heaviest mass per unit area than for the calico with the lightest mass per unit area. For the calicos with the medium and heaviest mass per unit area, the distance the blood spread laterally at impact, which increased with the increase in impact velocity, had a greater influence on the dry bloodstain area than the amount of wicking.

© 2019 Elsevier B.V. All rights reserved.

1. Introduction

Although bloodstain pattern analysis (BPA) has been used by crime scene investigators for over a century [1], questions have been raised on the scientific validity of the work [2]. The premise of BPA is that the pattern that blood creates when impacting a surface will enable the observer to gain an idea of the events which occurred to cause the bloodshed. However, the wide variety of creation mechanisms, drop sizes, impact velocities and target surfaces indicate the complexity of BPA [3]. The reliability of pattern classification of five bloodstain patterns on non-absorbent rigid surfaces [4] and fabric surfaces [5] by expert BPA analysts has been considered. On non-absorbent surfaces

incorrect classifications were made 13.1% of the time [4] and on fabric surfaces incorrect classifications were made 23.4% of the time [5].

As such, more research is being undertaken on the understanding of the interaction of blood with a variety of surfaces. Work has been carried out on non-absorbent surfaces (e.g. steel and plastic [6]) and partially absorbent surfaces (e.g. paper and wood [7–9]). Equations have resulted that use the bloodstain size and number of spines to back-calculate the impact velocity and assist in determination of the origin of the bloodstain [7–9].

Bloodstains on household and clothing fabrics often found at crime scenes are also being researched. To understand bloodstains on fabrics, it is important to consider wetting and wicking. Wetting and wicking are the mechanisms by which liquids move into and through a fabric [10]. Wetting occurs when the surface energy of a solid overcomes the surface tension of a liquid, allowing the liquid to spread on the surface [10]. Once a fabric has been wetted, wicking can occur. Wicking is the spontaneous transport of a liquid into a porous system by capillary forces. The rate at which the

* Corresponding author.

E-mail address: c.knock@cranfield.ac.uk (C. Knock).

¹ Present address: Defence and Security Accelerator, Porton Down, Salisbury, Wiltshire, SN4 0PQ, United Kingdom.

wicking occurs is dependent on the dimensions of the capillaries within the substrate, and the viscosity of the liquid [11].

Fibre content and fabric structure affect the wetting and wicking properties of a fabric [12,13]. A 65% polyester/35% cotton plain woven fabric produced larger bloodstains than either 100% cotton or 100% polyester plain woven fabrics. De Castro et al. [12,13] hypothesised that this may be in part due to the random mixture of cotton staple and cut polyester fibres which are spun together in a blend. This may have created larger interstitial spaces which resulted in more capillary action. Differences in capillary forces within 100% cotton plain woven and single jersey knitted fabrics may have resulted in the larger parent bloodstain area for the former [12].

When otherwise identical 100% cotton plain weave fabrics were manufactured from yarns which were either ring, rotor open end or Murata vortex air jet spun, porcine blood wicked only into the fabric woven from ring spun yarn [14]. When porcine blood was dropped vertically on to a commercially woven bed sheet, the elliptical bloodstains created were attributed to the warp yarns being ring spun, which wicked blood, and the weft yarns being Murata vortex spun, which did not. Therefore, even fabrics which appear identical may not result in similar bloodstains if the yarn manufacturing technique is different.

Scanning bloodstains with the use of a micro computed tomography (μ CT) scanner provided a greater insight into the internal structure of bloodstains on fabric [15]. For 100% cotton rib knit fabric sideways wicking (i.e. wicking along the yarns in the length and width of the fabric) dominated at the fastest impact velocity (5.3 ms^{-1}), resulting in larger, shallower bloodstains [15]. However, for 100% cotton drill fabric, little variation was seen as the velocity increased from 2.9 ms^{-1} to 5.3 ms^{-1} . A suggested explanation was that the small capillary spaces for the drill fabric resulted in the blood not spreading regardless of velocity.

Previous work has had inconsistent methodology which precludes the ability to compare and conglomerate the research. There is often inconsistency in the treatment of the fabric prior to experimentation, for example not stated [16,17], from a second-hand store so unknown [18] and sometimes laundered, although not always for the same number of cycles [19,20]. In a number of articles, the fabric properties (e.g. mass per unit area, thickness, sett, yarn linear density and twist) are not provided [16,17,19,21].

Whilst work has been published on the effects of fabric and fibre content on bloodstain morphology, the effect of mass per unit area has not been extensively studied. The aim of the current work was to understand the effects of fabric mass per unit area and blood impact velocity on the resultant parent bloodstain formed on three 100% cotton plain woven fabrics.

2. Materials and methods

2.1. Materials

To ensure the research was relevant to BPA, the fabrics used were 'household textiles'. Three rolls of calico fabric (100% cotton, plain woven), each with a different mass per unit area (85.1 g/m^2 (light), 163.5 g/m^2 (medium) and 224 g/m^2 (heavy)) were obtained from a fabric supplier² in order to study the effect of the different mass per unit areas on passive bloodstains (Table 1).

Dimensionally stable fabrics were created by washing the fabrics for six cycles in a domestic washing machine³ before line drying [22]. The fabrics were ironed under the same conditions

Table 1
Mean fabric properties and standard deviations where available (n=5).

	Light calico		Medium calico		Heavy calico	
Yarn type	Ring spun		Ring spun		Ring spun	
	Warp:	Weft:	Warp:	Weft:	Warp:	Weft:
Thickness (mm)	0.38 ± 0.03		0.46 ± 0.02		0.56 ± 0.03	
Mass per unit area (g/m^2)	85.1 ± 1.54		163.5 ± 2.26		224.6 ± 1.56	
Sett (yarns per 10 mm)	27×23		25×26		26×26	
Twist (turns per m)	650	650	756	756	650	624
Linear density (tex)	14	18	33	31	43	47

using a PSP-202E digital steam press on the cotton setting to remove creases. $100\text{ mm} \times 100\text{ mm}$ specimens (n=90) were cut from the fabrics, minimising repetition of warp and weft yarns, and were conditioned to $20 \pm 2^\circ\text{C}$ and $65 \pm 4\%$ R.H. for 24 h [23].

Fabric thickness (mm) [24], mass per unit area (g/m^2) [25] and sett [26] were measured. Yarn linear density was estimated by the removal of ten 1 m long yarns from the fabric and weighing them using an Oxford A2204 balance accurate to four decimal places. The twist level and yarn type were provided by the fabric supplier⁴ (Table 1). SEM images of the fabrics at $50\times$ magnification and the warp and weft yarns at $75\times$ magnification are available in the electronic Supplementary material.

Defibrinated horse blood sourced from Southern Group Laboratory⁵ was used to create the bloodstains. The blood was stored below 4°C , and used within one week of delivery.

2.2. Method

The horse blood was heated to 37°C in a water bath to simulate a blood-letting event at body temperature. Blood drops were formed in a Pasteur pipette and dropped from six different heights onto the fabrics, which were placed on a hard plastic surface. Blood was dropped from each height sequentially, but the order of specimens within a drop height was randomised. All drops were filmed using a Phantom V12 high-speed video (6273 fps and exposure $70\text{ }\mu\text{s}$). The high-speed video was subsequently analysed using Phantom Camera Control software⁶ to measure the droplet diameter and impact velocity for each drop height (Table 2). The mean diameter of the drops for all experiments was $3.3 \pm 0.17\text{ mm}$. Five repeats were taken at each velocity on each fabric resulting in a total of 90 specimens.

Bloodstains were photographed using a Nikon D3300 camera under the following conditions: wet ($\leq 30\text{ s}$ following the drop event) and dry on the technical face and on the technical rear of the fabric ($\geq 24\text{ h}$ later).

Dry specimens were analysed using a Nikon XTH225 micro Computed Tomography (μ CT) scanner⁷ (Table 3). For the μ CT scans, the fabric specimens were cropped to a width just greater than the parent bloodstain to increase the resolution of the scans, and mounted on a foam block. Foam was used as it was a different density from the fabric, and so the scanned image of the foam could easily be removed from the CT data during post-processing. The μ CT scanner was used to investigate the internal structure of the bloodstains as materials of different densities attenuate X-rays

⁴ Whaley's Bradford Ltd, Harris Court, Great Horton, Bradford, West Yorkshire, BD7 4EQ <http://www.whaleys-bradford.ltd.uk/>.

⁵ E-H Cavendish Courtyard, Sallow Road, Weldon North Industrial Estate, Corby, Northants www.sglab.co.uk.

⁶ <https://www.phantomhighspeed.com/resourcesandsupport/phantomresources/pccsoftware> page accessed 27th September 2018.

⁷ Nikon Metrology UK, Tring Business Centre, Icknield Way, Tring, Hertfordshire, HP23 4JX.

² Whaley's Bradford Ltd, Harris Court, Great Horton, Bradford, West Yorkshire, BD7 4EQ <http://www.whaleys-bradford.ltd.uk/>.

³ Samsung Ecobubble at 40°C cotton cycle.

Table 2

The drop heights and subsequent velocities measured from the high-speed video.

Drop height (mm)	Mean velocity and standard deviation (ms^{-1})
200	1.7 ± 0.01
500	2.9 ± 0.06
1000	4.1 ± 0.04
1500	4.9 ± 0.04
2000	5.1 ± 0.2
2500	5.4 ± 0.2

differently. The iron in the blood is the densest material on the blood-soaked fabric, and therefore the iron-rich bloodstains can be seen as separate from the less dense fabric background.

The μCT data was manually reconstructed in CT pro 3D⁸ (Table 3). The reconstructed data was then analysed in VGStudio Max⁹ and a 2D image of the 3D reconstruction of the bloodstain saved. Two-dimensional cross-sections were saved with a slice distance of 0.05 mm. Cross sections were obtained through the depth of the fabric in the warp and weft directions (Fig. 1).

The densest areas in the CT scans, where there is the most iron present, can be seen as the brightest areas within the cross-sections and 2D image of the 3D reconstruction. Fig. 2 is a representation of the different ways in which the blood may be seen in the μCT cross-sections.

The areas of the wet and dry technical face and technical rear of the parent bloodstains were obtained using the in-built tools in ImageJ¹⁰. Briefly, the image was converted to binary so the parent bloodstain was black against the white background. The area of the bloodstain was measured using the 'analyse particles' function. The outline of the measured area was compared to the original photograph to ensure spatter not connected to the parent bloodstain was not included in the measurement.

Two specimens from each fabric and velocity combination were examined using a Hitachi SU3500 SEM with the EDAX TEAM microanalysis system¹¹ (15 kV, 60 Pa). Background images were taken of the fabric ($\times 50$) and of a yarn removed from the fabric ($\times 75$) as well as of the dry bloodstains ($\times 42$ and $\times 250$).

To determine whether the blood drop impact velocity or fabric mass per unit area had a statistically significant effect on the wet and dry bloodstain areas, an analysis of variance (ANOVA) (IBM SPSS statistics version 22) was carried out. Statistical results are only reported in the results section if significant. Tukey's HSD test identified which variables or levels contributed towards any significant effects. To ensure that these statistical tests were viable, equality of variances and normality of data were checked.

3. Results and discussion

The resultant bloodstains from the passive blood drops were examined to compare the interaction between the blood and the fabric among the different fabrics and velocities.

Overall, the light calico produced the largest mean dry bloodstain area, and the medium the smallest, although this is not true across all velocities (Fig. 3). For the medium and heavy calico, a straight line fitted to the mean data using a least square fit gave a strong correlation for both wet (medium: $R^2 = 0.98$; heavy: $R^2 = 0.92$) and dry (medium: $R^2 = 0.93$; heavy: $R^2 = 0.94$) bloodstain

area with velocity. The correlation was lower for the light calico (wet: $R^2 = 0.6$; dry: $R^2 = 0.74$). Univariate analysis of variance (ANOVA) revealed impact velocity affected wet bloodstain area ($F_{17,72} = 49.314$, $p \leq 0.01$) and dry bloodstain area ($F_{17,72} = 37.459$, $p \leq 0.01$), the details of which are given in Table 4.

The results showed four groupings of velocities (Tables 4 and 5). The specimens from 1.7 ms^{-1} had dry bloodstains which were small and dense, and so the specimens from this velocity were looked at separately from the other velocities. The specimens from 2.9 , 4.1 and 4.9 ms^{-1} were grouped together as all fabrics had a gradual increase in mean dry bloodstain area with velocity. The medium calico had the smallest mean dry bloodstain area and the light the largest. Within a fabric, the bloodstains appeared visually similar. The specimens from 5.1 ms^{-1} were looked at separately from the other velocities as the medium calico had the largest mean dry bloodstain area, and the light calico the smallest, which only occurred at this velocity. Lastly, the specimens from 5.4 ms^{-1} were also looked at separately from the other velocities. This velocity resulted in a large increase in mean dry bloodstain area for the light and heavy calicos.

3.1. Impact velocity 1.7 ms^{-1}

At an impact velocity of 1.7 ms^{-1} the blood spread laterally on the technical face of the fabric following the initial impact, with little satellite stain and ligament formation (Fig. 4a–c). The blood then retracted to form a small bloodstain (Fig. 5a).

The small distance the blood spread laterally at impact resulted in the blood remaining pooled on the surface of all fabrics in the wet bloodstain photographs (Fig. 5). The blood pooled on the surface of the fabric refers to the blood which remained on the surface of the fabric following impact, and then either wicked into the fabric or dried on the surface of the fabric.

A key finding in the current work was the effect of the differences between the light, and the medium and heavy calicos on the bloodstains resulting from the 1.7 ms^{-1} impacts. On the light calico the blood which was pooled on the surface of the fabric was likely to enter the inter-yarn spaces, as these were largest for the light calico owing to the differences in yarn linear density among the three fabrics. In the CT cross-sections (Fig. 6a and b), both the warp (marked 'A') and weft (marked 'B') yarns are soaked in iron-rich blood. Once the blood was pooled in the inter-yarn spaces, the blood would have been able to wick into the yarns from all sides, filling the intra-yarn spaces. The volume of blood on the fabric surface, and in the inter-yarn spaces, then provided a reservoir for the blood to wick along the yarns after wetting. The lower linear density of the warp yarns (14 tex) than the weft yarns (18 tex) increased the amount of wicking in the former (Figs. 6c, marked 'C' and 8 a marked 'A'). The lower yarn linear density meant less blood was required to wet the yarn, and then fill the volume of the yarn, so the blood was able to wick further.

On the medium and heavy calicos more blood dried on the surface of the fabric than for the light calico (Fig. 7a–c). Compared to the light calico, the higher yarn linear density and smaller inter-yarn spaces of the medium and heavy calico meant it was more difficult for the blood to fill the inter-yarn spaces and surround the yarns. The blood pooled on the surface of the fabric and then wicked vertically through the yarns under gravity from the technical face towards the technical rear. This resulted in both the warp (marked 'A') and weft (marked 'B') yarns being soaked in iron-rich blood (Fig. 8), with blood also remaining on the surface of the fabric (Fig. 8, marked 'C'). Although blood was unlikely to have penetrated the fabric as a result of the impact [27], the blood wicked through to the technical rear of the fabric prior to the bloodstain drying (Fig. 7e and f). Although the blood was in the intra-yarn spaces, it did not wick along the yarns to the same

⁸ CT pro is 3D CT reconstruction software [33].

⁹ VGStudio Max enables the visualisation, examination and processing of CT data [34].

¹⁰ ImageJ is a public domain Java image processing programme (<https://imagej.nih.gov/ij/docs/intro.html>) page accessed 27th September 2018.

¹¹ <https://www.edax.com/products/eds/team-eds-system-for-the-sem> Page accessed 27th September 2018.

Table 3

The values at which all three masses of calico were scanned in the micro CT scanner and reconstructed.

Scanning values						Reconstruction	
Target	Voltage (kV)	Current (μA)	Exposure (ms)	Projections	Frames per projection	Beam hardening	Noise reduction
Tungsten	120	30	500	1080	2	1	1

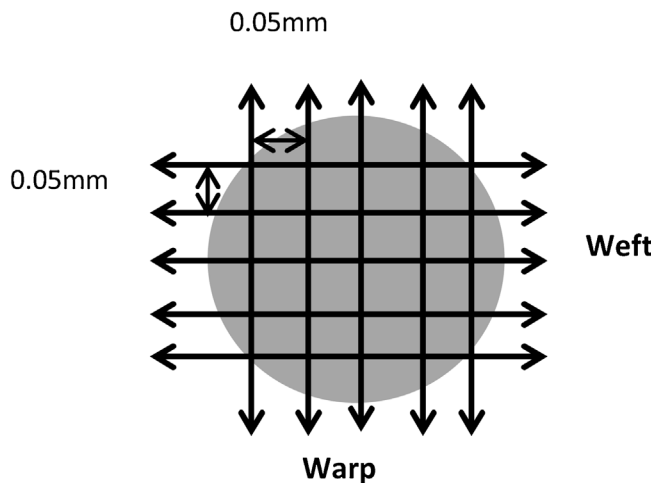


Fig. 1. Direction of the 2D images saved from the CT data. Cross-sections were saved at a slice distance of 0.05 mm in each of the warp and weft directions.

extent as the light calico. This was owing to the amount of time it would take to fully wet the high linear density yarns of the medium and heavy calico as the blood was only soaking through from the technical face of the fabric. When investigating spatter bloodstains on three 100% cotton knitted fabrics with different yarn linear densities, as with the current work on calico, it was found the smallest bloodstains were on the fabric with the greatest yarn linear density [28]. The greater the yarn linear density, the more air spaces there are between the fibres, therefore the more blood which is required to fully wet the yarns, before wicking can occur. The blood remaining on the surface of the fabric would dry before much wicking along the yarns was able to occur. 1.7 ms^{-1} is the only velocity where the heavy calico specimens had the smallest mean dry bloodstain area (Fig. 3). As the predominant method by which the bloodstains are being created on the medium and heavy calico at this velocity is wicking vertically into the fabric under gravity, the greater yarn linear density of the heavy than either the medium or light calico would reduce the ability of the blood to wick into the heavy calico.

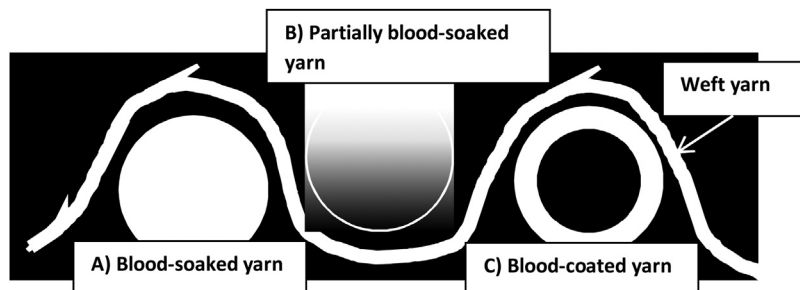


Fig. 2. A representation of the different ways the blood-soaked yarns appeared in the μCT cross-sections. (A) is a representation of a completely blood-soaked yarn, where the yarn was the same density throughout. (B) is a representation of a partially blood-soaked yarn, where there were some areas which were denser than others, and therefore where more iron is present (typically towards the technical face of the fabric). (C) is a representation of a blood-coated yarn, where the dense iron-rich blood was only present around the outside of the yarn, and the centre of the yarn remained blood free.

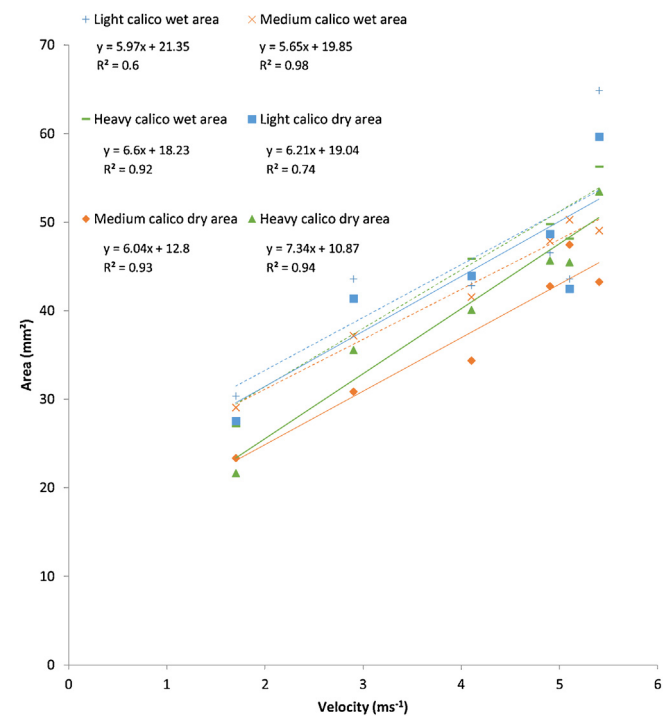


Fig. 3. Mean wet and dry bloodstain area at each velocity for all fabrics.

On all three fabrics for 1.7 ms^{-1} impacts the blood which remained on the surface of the fabric dried in the manner of the coffee ring effect (Fig. 8a–c, marked 'B') [29,30]. The coffee ring effect occurs in many colloidal fluids when the solutes move to the pinned edge of the liquid drop to compensate for evaporative losses [31]. This results in a higher concentration of particulates at the edge of the drop than the centre, and is evidenced by a ring of dense blood surrounding the parent bloodstain.

As a larger volume of blood remained on the surface of the medium and heavy calicos than the light calico, the coffee ring effect was more pronounced. The coffee ring effect occurred more extensively for 1.7 ms^{-1} impacts as blood pooled on the surface of all fabrics following impact and dried before wicking occurred.

Table 4

The mean bloodstain area and statistical differences among the fabrics (light: 85.1 g/m²; medium: 163.5 g/m²; heavy: 224.6 g/m²) for each velocity.

Velocity category (ms ⁻¹)	Mean dry bloodstain area and standard deviation (mm ²)	Statistics
1.7	L: 27.6 ± 4.4 M: 23.4 ± 4.7 H: 21.7 ± 3.2	Technical face wet and dry bloodstain areas statistically significantly smaller than all other velocities.
2.9	L: 41.4 ± 3.6 M: 30.9 ± 5.6 H: 35.6 ± 7.8	Technical face wet and dry bloodstain area for 2.9 ms ⁻¹ statistically significantly smaller than 4.9 ms ⁻¹ , 5.1 ms ⁻¹ and 5.4 ms ⁻¹ .
4.1	L: 44 ± 6.9 M: 34.4 ± 3.9 H: 40.1 ± 6.3	Technical face wet bloodstain area for 4.1 ms ⁻¹ and 4.9 ms ⁻¹ is statistically significantly smaller than 5.4 ms ⁻¹ . Technical face dry bloodstain area for 4.1 ms ⁻¹ statistically significantly smaller than 5.4 ms ⁻¹ .
4.9	L: 48.7 ± 12 M: 42.8 ± 5.7 H: 45.7 ± 4.5	Technical face wet bloodstain area for 4.9 ms ⁻¹ is statistically significantly smaller than 5.4 ms ⁻¹ .
5.1	L: 42.5 ± 3.4 M: 47.5 ± 8.8 H: 45.5 ± 4.3	Technical face wet and dry bloodstain area statistically significantly smaller than 5.4 ms ⁻¹ .
5.4	L: 59.7 ± 6.4 M: 43.3 ± 4.1 H: 53.5 ± 7.3	Technical face wet bloodstain area statistically significantly larger than all other velocities. Technical face dry bloodstain area statistically significantly larger than 1.7 ms ⁻¹ , 2.9 ms ⁻¹ , 4.1 ms ⁻¹ and 5.1 ms ⁻¹ .

Table 5

A summary of the way in which blood is interacting with each fabric (light: 85.1 g/m²; medium: 163.5 g/m²; heavy: 224.6 g/m²) for each velocity category.

Velocity category (ms ⁻¹)	Light calico	Medium calico	Heavy calico
1.7	<ul style="list-style-type: none"> - Blood pooled on the surface of the fabric when wet, filling the inter-yarn spaces (Fig. 5a) - Blood surrounded yarns and wicked into the yarns from all sides - Pooled blood provided a reservoir for blood to wick along the intra-yarn spaces (Fig. 6a and b) - Bloodstain dried in the manner of the coffee ring effect (Fig. 8a) 	<ul style="list-style-type: none"> - Blood remained pooled on the surface of the fabric (Fig. 5b and c) - Blood wicked vertically through the yarns under gravity - Only a small amount of wicking along the intra-yarn spaces - Large volume of blood dried on the surface of the fabric (Fig. 8b and c) 	
2.9, 4.1 and 4.9	<ul style="list-style-type: none"> - No wet blood pooled on the fabric technical face (Fig. 9a) - Blood penetrated the fabric at impact through to the technical rear (Fig. 9g) - Wicking occurred along the intra-yarn spaces and removed iron-rich blood from the centre of the bloodstain (Fig. 10a and b) - Very little blood dried on the surface of the fabric (Fig. 9d) 	<ul style="list-style-type: none"> - Blood remained pooled on the surface in specimens from 2.9 and 4.1 ms⁻¹ (Fig. 9b) - Blood wicked vertically into the warp and weft yarns (Fig. 10d and e) - Wicking along the intra-yarn spaces impeded owing to the greater twist than for the light and heavy calicos 	<ul style="list-style-type: none"> - Blood remaining pooled on the surface in specimens from 2.9 and 4.1 ms⁻¹ (Fig. 9c) - Blood dried before penetrating through the thickness of the yarns (Fig. 10 g and h) - A large volume of blood dried on the surface of the fabric (Fig. 9f)
5.1	<ul style="list-style-type: none"> - No wet blood pooled on the fabric technical face - Blood penetrated the yarns at impact – very little blood in the inter-yarn spaces (Fig. 11a–c) - With no blood pooled on the surface further wicking along the intra-yarn spaces could not take place. 	<ul style="list-style-type: none"> - No wet blood pooled on the fabric technical face - Blood penetrated the yarns at impact (Fig. 11d–f) - Blood penetrated through to the technical rear of the fabric (Fig. 12e) - Some wicking occurred along the intra-yarn spaces. 	<ul style="list-style-type: none"> - No wet blood pooled on the fabric technical face - Blood penetrated the yarns at impact (Fig. 11g–i) - Less blood available for lateral spreading - Greater yarn linear density of the heavy calico meant blood could not wick easily along the yarns
5.4	<ul style="list-style-type: none"> - No wet blood pooled on the fabric technical face (Fig. 13a) - Large amount of spreading on the technical face at impact - Penetration through to the technical rear at impact (Fig. 13g) - Blood wicked into the warp yarns, but only coated the weft yarns (Fig. 14a and b) - Once the blood was either in or around the yarns, it then wicked along the intra-yarn spaces. 	<ul style="list-style-type: none"> - Small amount of blood remained on the surface following impact (Fig. 13b) - Blood penetrated through to technical rear at impact (Fig. 13h) - Blood coating the warp and weft yarns (Fig. 14d and e) – Small amount of wicking occurred - Wicking limited owing to blood drying on the surface and the greater twist of the medium calico. 	<ul style="list-style-type: none"> - Small amount of blood remained on the surface following impact (Fig. 13c) - No penetration through to the technical rear of the fabric at impact (Fig. 13i) - Blood spread laterally across the surface of the fabric

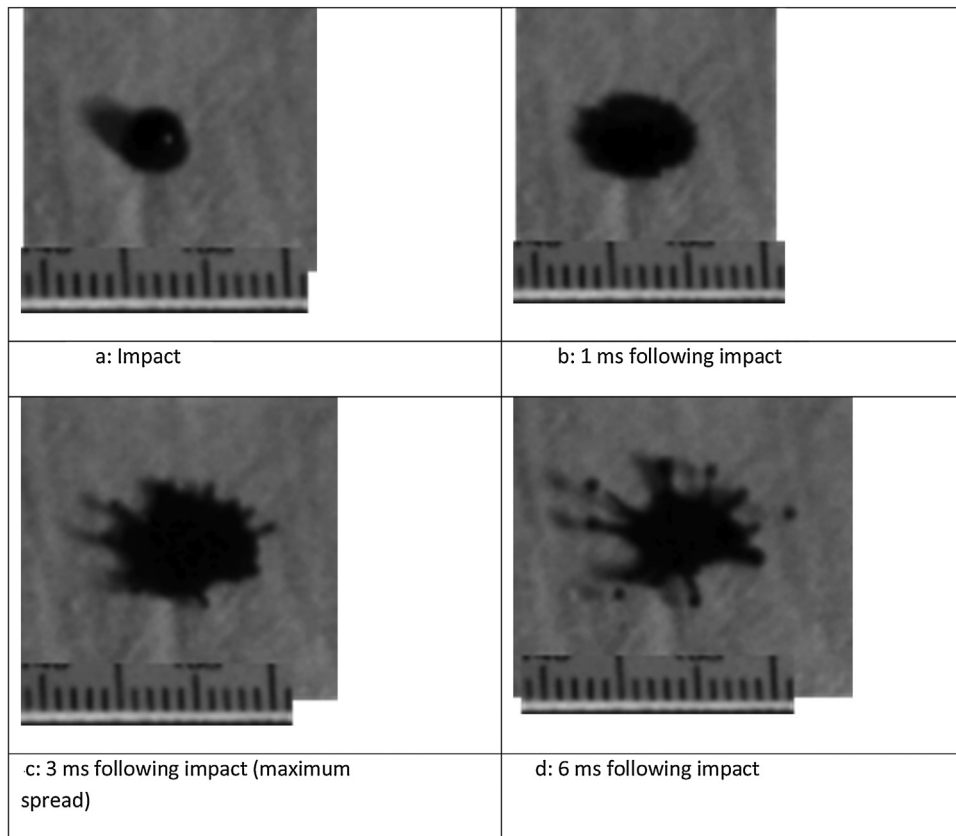


Fig. 4. Typical example of a blood drop impacting the light calico at 1.9 ms^{-1} (images from work undertaken for Ref. [27] but not used in the publication).

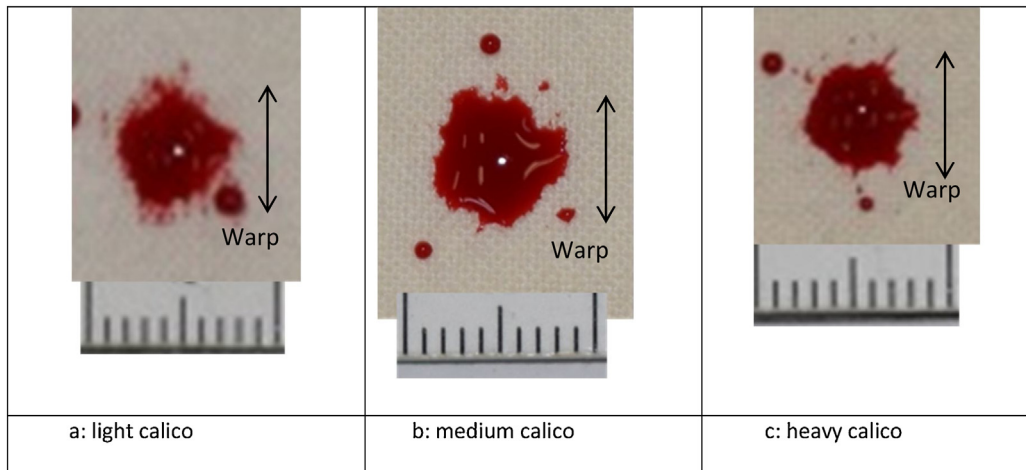


Fig. 5. Typical example of a wet bloodstain on each calico formed at 1.7 ms^{-1} . Scale is 10 mm.

3.2. Impact velocities 2.9 , 4.1 and 4.9 ms^{-1}

On the light calico there was a large increase in mean dry bloodstain area from 27.6 mm^2 at 1.7 ms^{-1} to 41.4 mm^2 at 2.9 ms^{-1} (Fig. 3) owing to the increase in lateral spreading following impact due to the increase in velocity. This increase in lateral spreading resulted in no blood remaining pooled on the surface of the light calico (Fig. 9a). The blood instead penetrated the yarns through to the technical rear of the light calico (Fig. 9g, marked 'A') some of which occurred closely following impact, with wicking further increasing the technical rear bloodstain area [27]. The amount of blood which penetrated to the technical rear following impact has

previously been found to increase with an increase in impact velocity from 1.9 ms^{-1} to 4.2 ms^{-1} (7.2 mm^2 – 18.6 mm^2) [27].

For the light calico, the CT scans of all the bloodstains at this velocity showed neither the warp nor weft yarns contained a large amount of iron-rich blood (Fig. 10a and b), with only a patchy area in the centre of the bloodstain (marked 'A'). At the edge of the bloodstain there is iron-rich blood primarily on the warp yarns (marked 'B'). Once the blood penetrated the intra-yarn spaces of the light calico, wicking occurred along them to remove the particulates (red blood cells, white blood cells and platelets) from the centre of the bloodstain towards the edge, removing any blood which was originally pooled in the inter-yarn spaces (Fig. 10c,

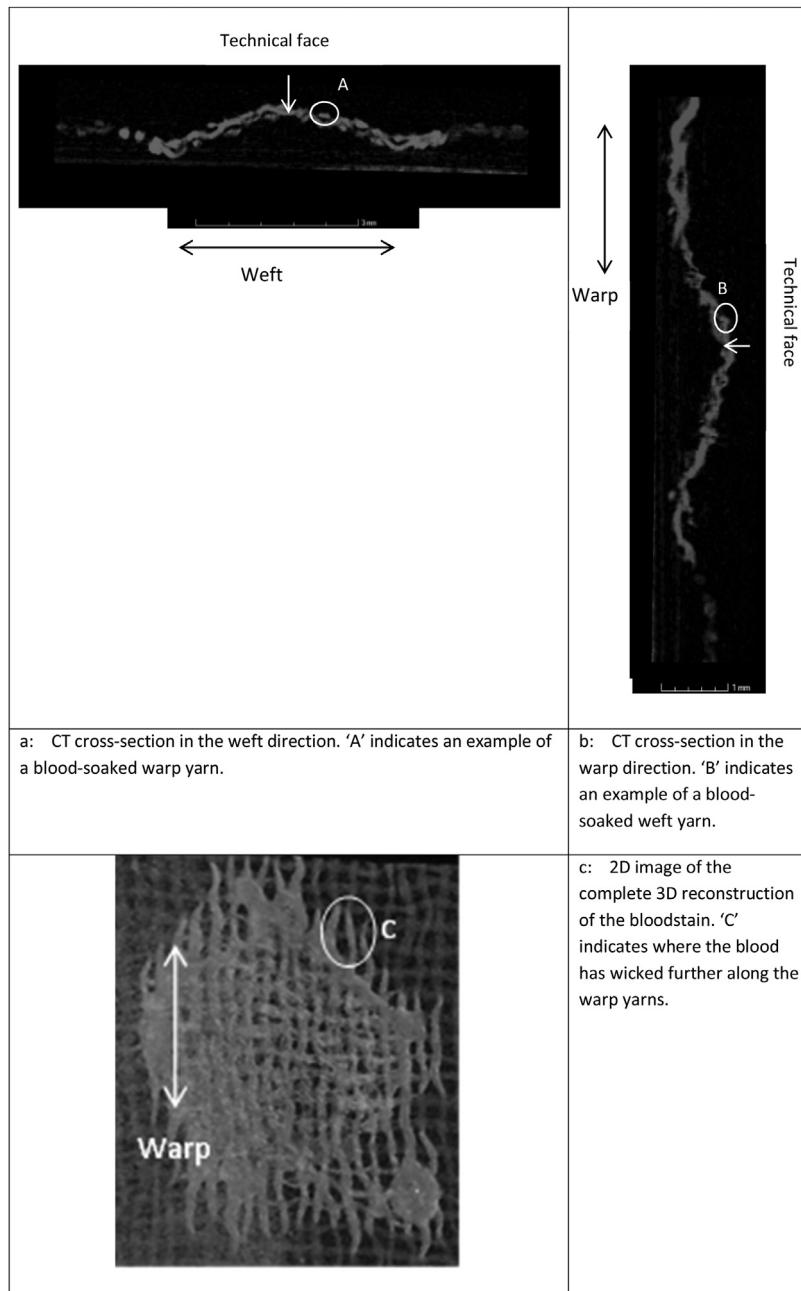


Fig. 6. The CT data from a typical example of a light calico specimen formed at 1.7 ms^{-1} .

marked 'C'). Any particulates which remained in the centre of the bloodstain were spread out owing to the larger dry bloodstain areas at these velocities than at 1.7 ms^{-1} . The amount of wicking which was occurring at 2.9 , 4.1 and 4.9 ms^{-1} on the light calico resulted in similar mean dry bloodstain areas at these three velocities (41.4 , 44.0 and 48.7 mm^2 respectively) and reduced the correlation of mean dry bloodstain area and velocity.

The dry bloodstains formed on the light (thinnest) calico specimens from impact velocities of 2.9 , 4.1 and 4.9 ms^{-1} had a larger mean area than the medium and heavy calico specimens (Fig. 3, Table 4). However, there was only one statistically significant difference in dry bloodstain area among the fabrics at any of these three velocities. From an impact velocity of 2.9 ms^{-1} ($F_{2,12} = 3.951$, $p \leq 0.05$), the light calico was statistically significantly larger than the medium calico. A larger bloodstain on a thinner fabric was also seen when bloodstains on a blend (65% polyester/35% cotton) plain

woven fabric were compared to those on 100% cotton and 100% polyester fabrics which had greater thickness and mass per unit area [12]. Although fibre content may also have had an effect in this previous work, it was suggested that the large bloodstain size was caused by the blood spreading laterally over the fabric, rather than over and through the fabric [12].

For the medium and heavy calico, blood remained pooled on the surface of the fabric when the blood impacted at a velocity of 2.9 ms^{-1} or 4.1 ms^{-1} (Fig. 9b and c). At an impact velocity of 4.9 ms^{-1} no blood remained pooled on the fabric surface owing to the greater distance the blood spread laterally at impact. The increase in lateral spreading also increased the mean dry bloodstain area with velocity (Fig. 3, Table 4).

Although the blood could not penetrate the medium calico as easily as the light calico owing to the smaller inter-yarn spaces, all the CT scans of the medium calico bloodstains at this velocity showed

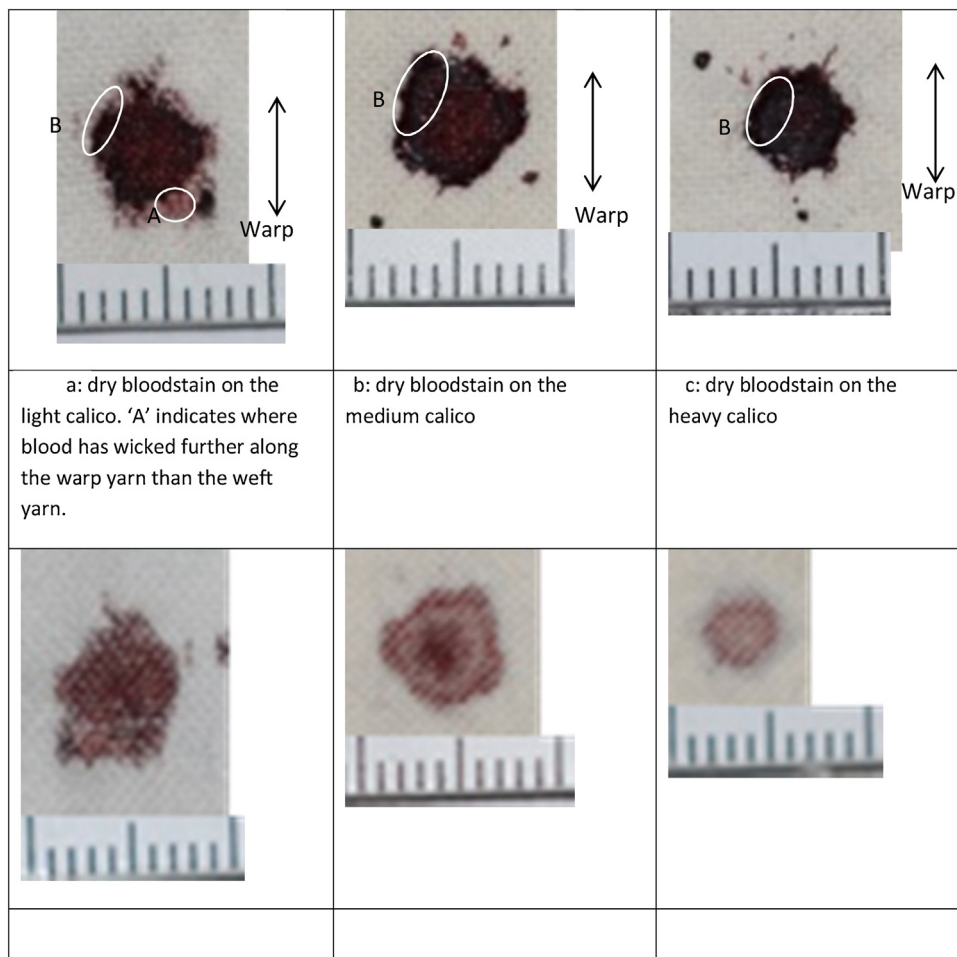


Fig. 7. A typical example of a dry bloodstain on each calico formed at 1.7 ms^{-1} . 'B' indicates the coffee ring effect in part of the bloodstains. Scale is 10 mm.

iron-rich blood did wick into both the warp and weft yarns. This occurred primarily on the sections of the yarns which were on the technical face of the fabric (Fig. 10d and e, marked 'A'). The blood was therefore penetrating the yarns from the reservoir pooled on the surface of the fabric. However, the high twist level of the medium calico (756/756) compared to the heavy calico (650/624) impeded the wicking of the blood along the intra-yarn spaces, resulting in the smallest mean dry bloodstain area at each of these velocities.

The μCT cross-sections for all the heavy calico specimens at this velocity indicated very little iron-rich blood in the centre of the bloodstain (Fig. 10g and h). Any iron-rich blood in the centre of the bloodstain (marked 'A') is primarily on the warp yarns, and the blood has not soaked all the way through to the centre of the yarns (Fig. 10g, 'A'). This is possibly due to the higher linear density for the heavy than the light and medium calicos. The blood dried before penetrating to the centre of the yarns, shown by the volume of dry blood which remained on the surface of the fabric (Figs. 9f, marked 'A', Fig. 10i marked 'B'), filling the inter-yarn spaces (Fig. 10i, marked 'C'). At an impact velocity of 4.2 ms^{-1} it has previously been found that no blood penetrated through to the technical rear of the heavy calico at impact, while blood did penetrate both the medium and light calicos [27].

3.3. Impact velocity 5.1 ms^{-1}

5.1 ms^{-1} was the only velocity where the largest mean dry bloodstain area was on the medium calico, and the smallest on the light calico (Fig. 3, Table 4). The difference in mean dry bloodstain

area at 5.1 ms^{-1} was not statistically significant (the difference between the medium and light calico was only 5 mm^2).

For all specimens from an impact velocity of 5.1 ms^{-1} both the warp (marked 'A') and weft (marked 'B') yarns were almost completely soaked in iron-rich blood (Fig. 11a, b, d, e, g and h), where the full shape of the yarn is seen (Fig. 2). Less blood was visible on the surface of the yarns at 5.1 ms^{-1} (Fig. 11c, f, i) than at 4.1 ms^{-1} (Fig. 10c, f, i). As the blood was able to penetrate the intra-yarn spaces for all three fabrics at this velocity, regardless of the yarn linear density, this would suggest that the increase in velocity to 5.1 ms^{-1} enabled the blood to penetrate into the yarns at impact, filling the intra-yarn spaces. Evidence for a higher velocity forcing blood to penetrate into the intra- and inter- yarn spaces has previously been seen when passive bloodstains on a 100% cotton rib knit fabric were examined using a μCT scanner [15]. In this previous work, the bloodstains formed from a velocity of 5.3 ms^{-1} reached their maximum extent closer to the technical face of the fabric than the middle velocity (4.5 ms^{-1}), with a mean maximum cross-sectional area larger than either of the other two velocities investigated in this previous work ($3.2, 4.5 \text{ ms}^{-1}$) [15]. The higher velocity appeared to therefore be forcing the blood into the intra- and inter-yarn spaces, as occurred on the calico fabrics from an impact velocity of 5.1 ms^{-1} .

On the light calico the mean dry bloodstain area decreased from 48.7 mm^2 at 4.9 ms^{-1} to 42.5 mm^2 at 5.1 ms^{-1} . The coefficient of variation (CV) for the light calico at 5.1 ms^{-1} (8%) was lower than at 4.9 ms^{-1} (25%). This was possibly due to a greater amount of wicking at 4.9 ms^{-1} increasing the variability in the dry bloodstain area. The amount of wicking in a specimen would be dependent on variations within the

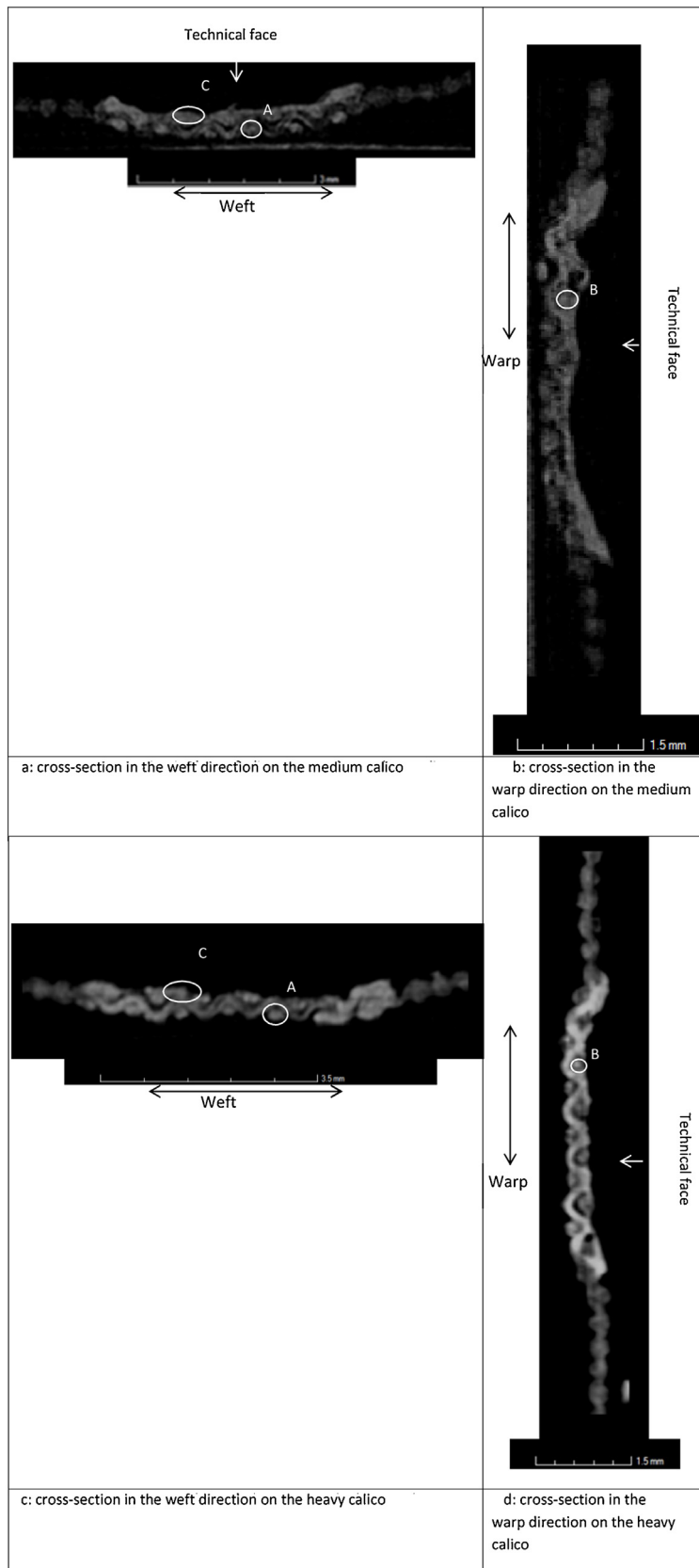


Fig. 8. A typical example of a cross-section in the warp and weft directions on the medium and heavy calico formed at 1.7 ms^{-1} . 'A' indicates an example blood-soaked warp yarn, 'B' an example blood-soaked weft yarn and 'C' the blood remaining on the surface of the fabric.

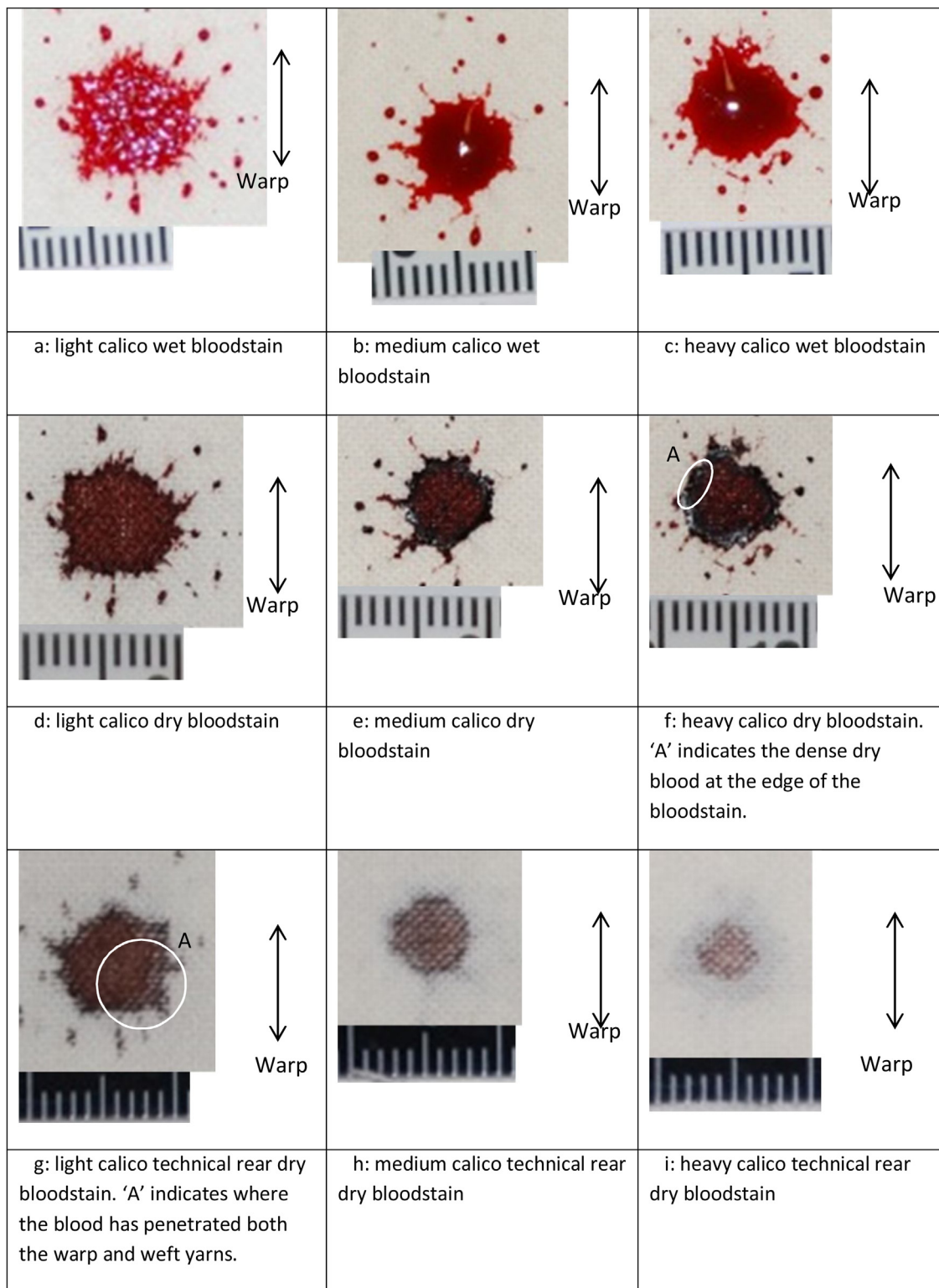


Fig. 9. A typical example of a technical face wet and dry and technical rear dry bloodstain on each calico formed at 4.1 ms^{-1} . Scale is 10 mm.

fabric and yarns [32] and therefore would differ between specimens. When the area of the bloodstain is more dependent on wicking than on the distance the blood spread laterally at impact, greater variability among specimens within that velocity will be seen. The reduced wicking at 5.1 ms^{-1} , indicated by less variability among specimens, resulted in the smaller mean dry bloodstain area at this velocity.

The mean dry bloodstain area on the heavy calico decreased slightly despite the increase in impact velocity from 45.7 mm^2 at 4.9 ms^{-1} to 45.5 mm^2 at 5.1 ms^{-1} . There is little evidence of dense blood on the surface of the heavy calico in the dry bloodstains (Fig. 12c). This was due to the blood penetrating the yarns rather than remaining on the surface of the fabric. Although the blood was

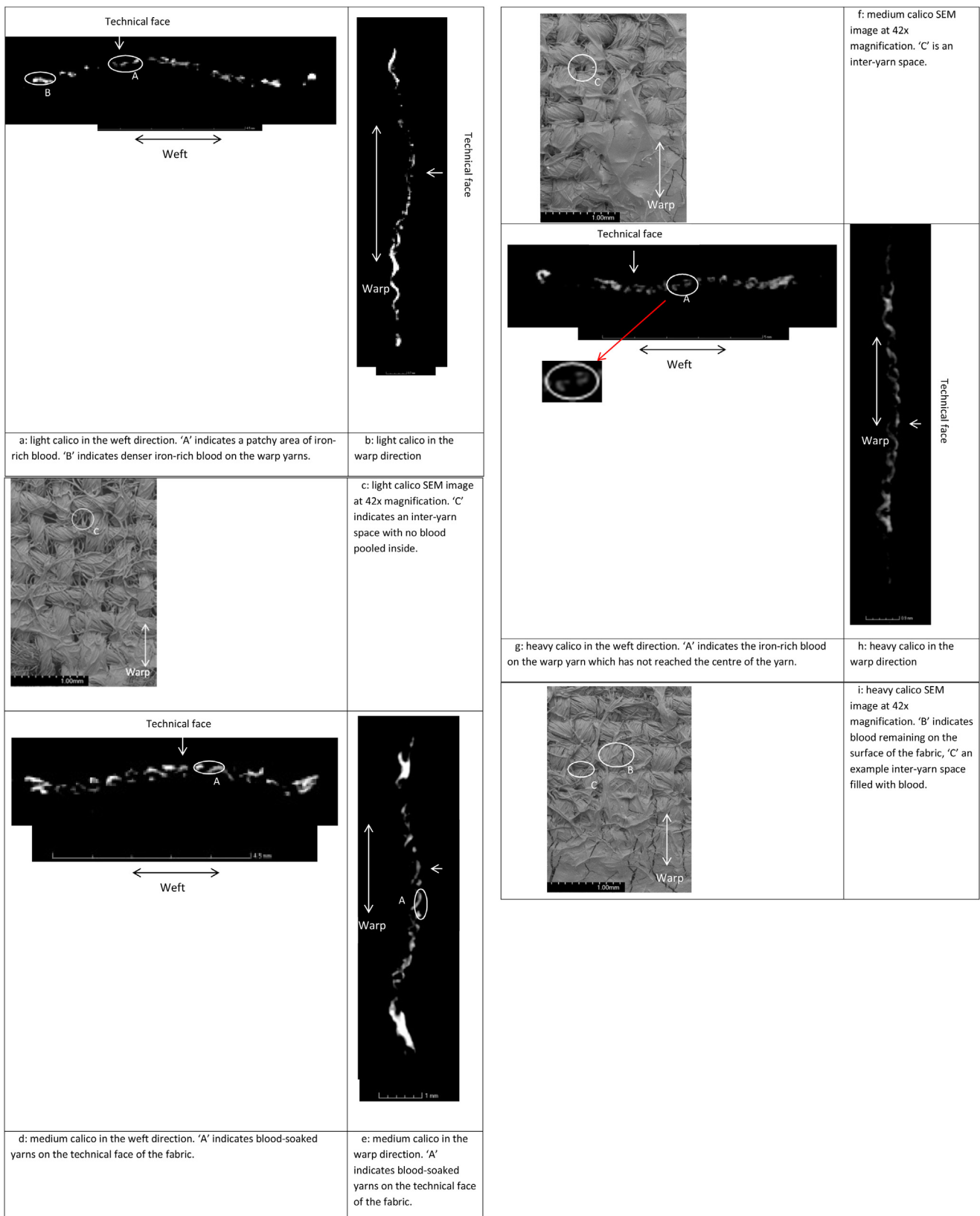


Fig. 10. A typical example of a CT cross section in the warp and weft directions and an SEM image ($\times 42$) on each calico formed at 4.1 ms^{-1} .

then in the intra-yarn spaces, the high yarn linear density of the heavy calico precluded wicking.

The medium calico was the only fabric where the mean dry bloodstain area increased with the increase in velocity from 42.8

mm^2 at 4.9 ms^{-1} to 47.5 mm^2 at 5.1 ms^{-1} . The CV also increased from 13% to 19% suggesting a greater amount of wicking was occurring, as this would increase the inconsistency of the dry bloodstain area among specimens [32]. The largest technical rear

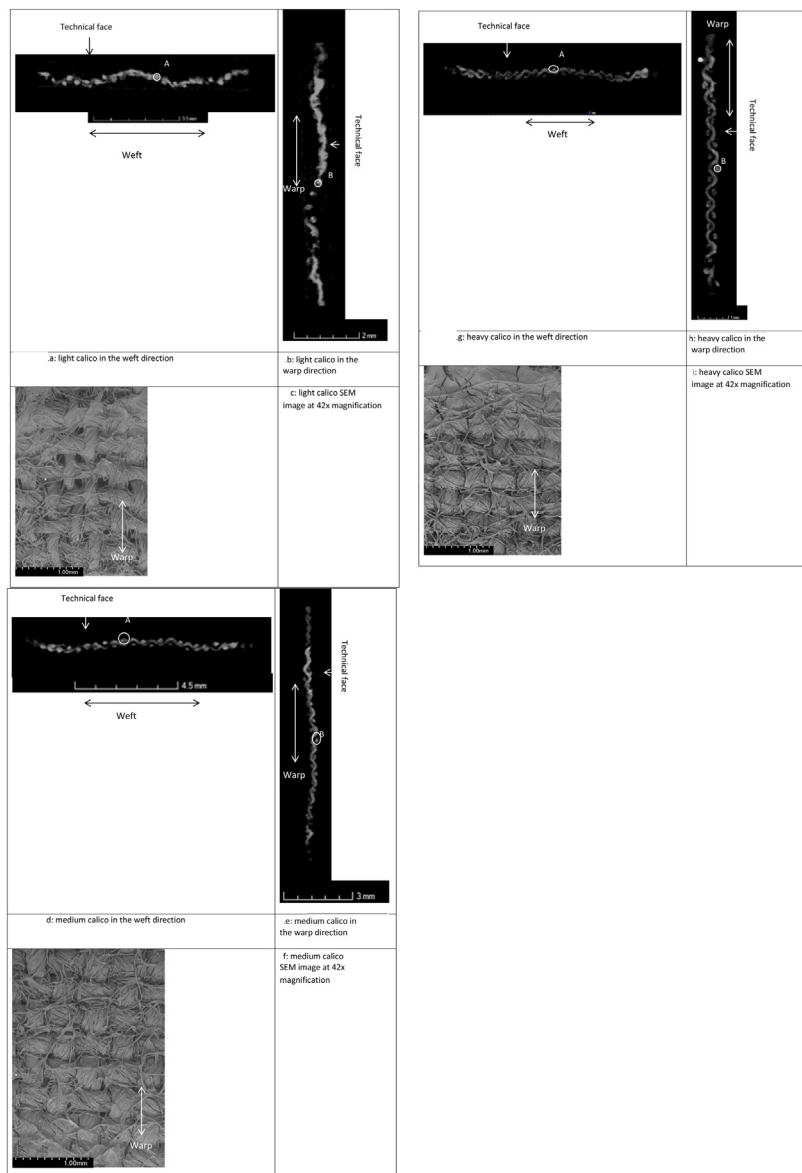


Fig. 11. A typical example of a CT cross section in the warp and weft directions and an SEM image ($\times 42$) on each calico formed at 5.1 ms^{-1} . 'A' indicates the blood soaked warp yarns, and 'B' the blood soaked weft yarns.

bloodstain on the medium calico was seen on the specimens from a velocity of 5.1 ms^{-1} (Fig. 12e). Blood penetrated the yarns through to the technical rear of the medium calico across the entire bloodstain and then wicked along the yarns as the blood was already in the intra-yarn spaces. The lower yarn linear density for the medium than the heavy calico meant more wicking occurred in the former.

3.4. Impact velocity 5.4 ms^{-1}

The light calico specimens had the largest mean dry bloodstain area and the medium the smallest from a velocity of 5.4 ms^{-1} (Fig. 3, Table 4). The difference in mean dry bloodstain area among fabrics at 5.4 ms^{-1} was statistically significantly different ($F_{2,12} = 9.32, p \leq 0.01$). The mean dry bloodstain area for the light calico (59.7 mm^2) was significantly larger than the medium (43.3 mm^2). The mean dry bloodstain area for the heavy calico (53.5 mm^2) was not significantly different.

For the light calico specimens from 5.4 ms^{-1} , the blood spread a large distance following impact as shown in the increase in mean

wet bloodstain area from 43.6 mm^2 at 5.1 ms^{-1} to 64.9 mm^2 at 5.4 ms^{-1} . The distance the blood drop spread on the surface of the fabric following impact depended on the kinetic energy at impact. The kinetic energy was converted to surface energy causing the spreading [20]. The increase in impact velocity from 1.7 ms^{-1} to 5.4 ms^{-1} resulted in an increase in kinetic energy of over 900%, hence resulting in more spreading on the surface of the fabric.

No blood remained pooled on the surface of the light calico specimens from 5.4 ms^{-1} impacts (Fig. 13a). A large amount of blood penetrated through to the technical rear of the fabric (Fig. 13g). Iron-rich blood penetrated through the entire thickness of the warp yarns (Fig. 14a, marked 'A') while only coating the weft yarns (Fig. 14b, marked 'B'). The predilection for the warp yarns owing to their lower linear density (14 compared to 18 tex) can be seen around the edge of the dry technical face (Fig. 13d marked 'A') and technical rear (Fig. 13g marked 'A') bloodstain and the 2D image of the 3D CT reconstruction (Fig. 13j). As the warp yarn on the light calico was soaked in blood it was possible for the blood to wick along the intra-yarn spaces within the yarns, increasing the bloodstain area.

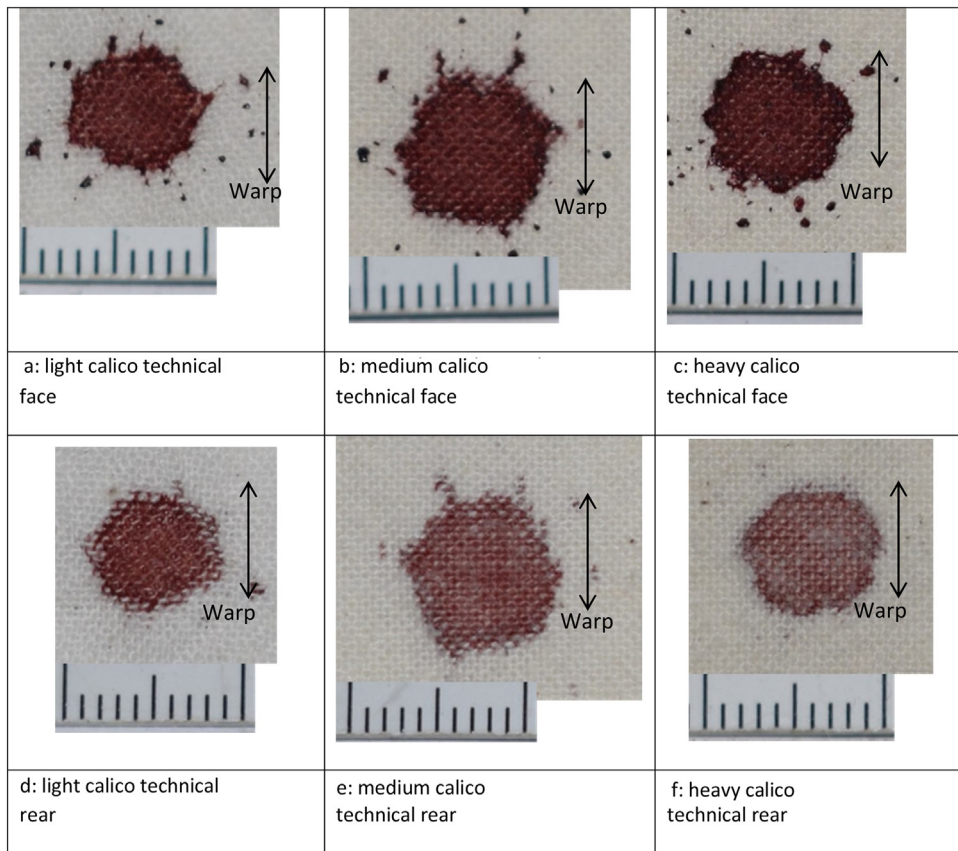


Fig. 12. A typical example of a dry technical face and technical rear bloodstain on each calico formed at 5.1 ms^{-1} . Scale is 10 mm.

The mean technical rear bloodstain area for the medium calico decreased from 27.8 mm^2 at 5.1 ms^{-1} to 15.1 mm^2 at 5.4 ms^{-1} . However, the specimens from an impact velocity of 5.4 ms^{-1} were the only specimens on the medium calico where the blood completely penetrated to the technical rear of the fabric (Fig. 13h, marked 'B'). The blood coated the warp and weft yarns (Fig. 13d and e, marked 'A') rather than penetrating through to the centre of them. Therefore, the blood on the technical rear of the medium calico was forced through the inter-yarn spaces and around the yarns at impact, as the higher twist level of the medium calico reduced the ability of the blood to penetrate into the yarns themselves. Some blood also remained pooled on the surface of the medium calico (Fig. 13b). The blood on the surface dried before being able to fully wick into the intra-yarn spaces, therefore reducing the amount of wicking which occurred along them. The greater yarn twist of the medium than the heavy and the light calicos reduced the ability of the blood to wick into and along the intra-yarn spaces, reducing the dry bloodstain area.

For the heavy, as for the medium calico, iron-rich blood coated both the warp and weft yarns (Fig. 14g and h), although blood did not completely penetrate through to the technical rear of the fabric (compare Fig. 13i–h). The blood remained more on the surface of the heavy calico than either the medium or light calicos owing to the higher yarn linear density. This is evidenced by a greater amount of iron-rich blood towards the technical face of the fabric in the μCT cross-sections (Fig. 14g and h) and the ring of dense blood which occurred on the surface of the fabric (Fig. 13l). Therefore, with the increase in impact velocity to 5.4 ms^{-1} the blood spread laterally across the surface of the heavy calico, as opposed to penetrating through to the technical rear of the fabric

as for the medium calico. This resulted in a larger mean dry bloodstain area for the heavy than the medium calico.

3.5. All velocities

A summary of the differences in results between the different impact velocities and fabrics is given in Table 5.

4. Conclusions

Passive bloodstains were created on three mass per unit areas (light: 85 g/m^2 , medium: 164 g/m^2 and heavy: 225 g/m^2) of 100% cotton plain woven calico. Six drop heights were used, resulting in six impact velocities ($1.7, 2.9, 4.1, 4.9, 5.1$ and 5.4 ms^{-1}). The use of μCT enabled the internal structure of the bloodstains to be assessed. This provided an understanding of where the blood was within the bloodstain, and whether it had penetrated or coated the yarns, which was imperative to understanding the interaction of the blood and the fabric.

The bloodstains varied depending on the type of fabric and the velocity with which the blood impacted. Overall, dry bloodstain area increased with impact velocity, although this was not consistent across all three fabrics. The light calico generally had the largest mean dry bloodstain area but had a lower correlation with velocity. This was due to the low yarn linear density of the light calico which reduced the volume the blood had to fill; therefore the blood wicked further along the yarns. The correlation with velocity was greater for the medium and heavy calicos. Less wicking along the intra-yarn spaces occurred, and so the dry bloodstain area was more dependent on the distance the blood spread laterally following impact, which increased with the

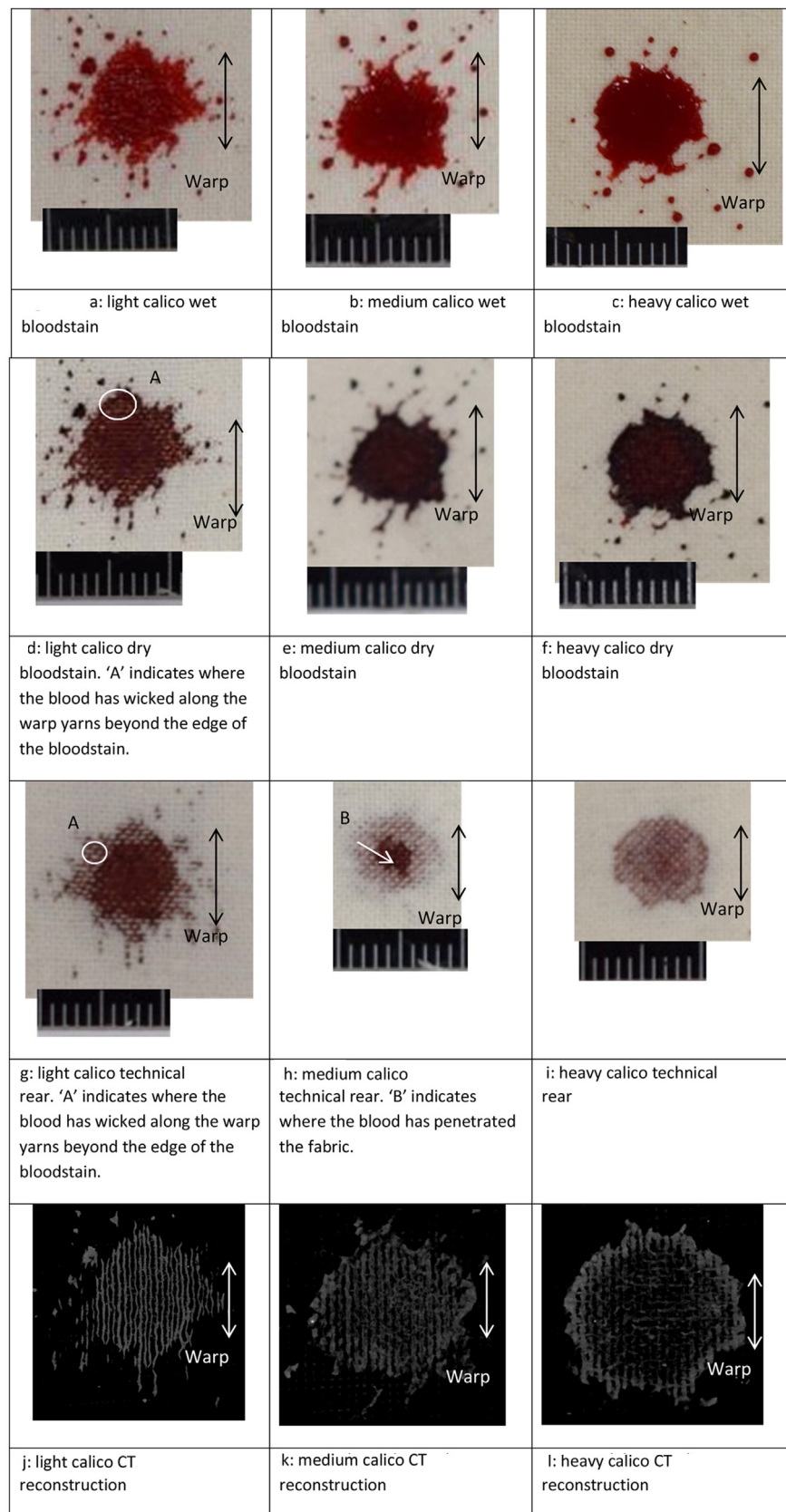


Fig. 13. A typical example of a wet and dry technical face and dry technical rear bloodstain (scale: 10 mm) and 2D of the 3D CT reconstruction on each calico formed at 5.4 ms^{-1} .

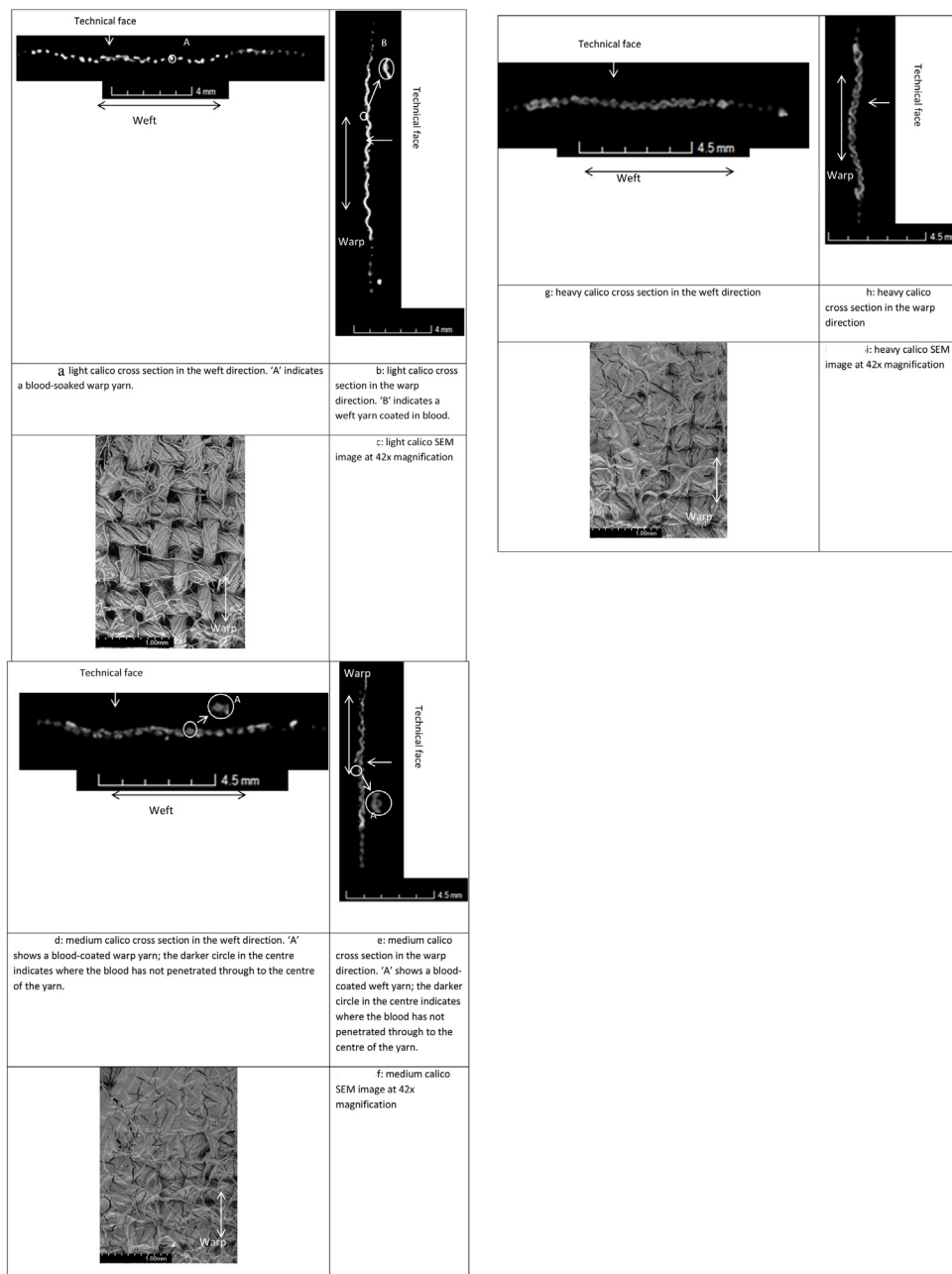


Fig. 14. A typical example of a CT cross section in the warp and weft directions and an SEM image ($\times 42$) on each calico formed at 5.4 ms^{-1} .

increase in impact velocity. At a slow impact velocity (1.7 ms^{-1}) the blood pooled on the surface of the fabric wicked slowly into the warp and weft yarns under gravity, while at a faster impact velocity (e.g. 4.1 ms^{-1}) the particulates were more spread out within the bloodstain, resulting in very different CT scans between fast and slow impact velocities. This is important to note for forensic science, as in some circumstances it may be possible to ascertain something of the area of origin of the bloodstain on the basis of a fast or slow impact velocity.

For forensic science, it is also important to note that fabric mass per unit area needs to be taken into account when analysing bloodstains on fabrics. When comparing bloodstains between two fabrics of identical fibre content and weave structure, the fabric

with the lower mass per unit area may produce a larger bloodstain than that of the higher mass per unit area irrespective of the velocity with which the blood impacted.

Ethical statement

All applicable international, national and institutional guidelines for the care and use of animals were followed.

Declarations of interest

None.

Appendix A. Supplementary data

Supplementary material related to this article can be found, in the online version, at doi:<https://doi.org/10.1016/j.forsciint.2019.05.001>.

References

- [1] S.H. James, P.E. Kish, T.P. Sutton, *Principles of Bloodstain Pattern Analysis: Theory and Practice*, CRC Press, Florida, 2005.
- [2] National Research Council, Strengthening Forensic Science in the United States: A Path Forward, The National Academic Press, Washington, D.C., 2009 Available on line at <https://www.ncjrs.gov/pdffiles1/nij/grants/228091.pdf> (accessed 16/05/2019).
- [3] T. Bevel, R.M. Gardner, *Blood Pattern Analysis with an Introduction to Crime Scene Reconstruction*, third ed., CRC Press, Florida, 2008.
- [4] M.C. Taylor, T.L. Laber, P.E. Kish, G. Owens, N.K.P. Osborne, M. Sc, G. Owens, N.K. P. Osborne, The reliability of pattern classification in bloodstain pattern analysis, part 1: bloodstain patterns on rigid non-absorbent surfaces, *J. Forensic Sci.* (2016) 1–6, doi:<http://dx.doi.org/10.1111/1556-4029.13091>.
- [5] M.C. Taylor, T.L. Laber, P.E. Kish, G. Owens, N.K.P. Osborne, The reliability of pattern classification in bloodstain pattern analysis, part 2: bloodstain patterns on fabric surfaces, *J. Forensic Sci.* 61 (2016) 1461–1466, doi:<http://dx.doi.org/10.1111/1556-4029.13091>.
- [6] B.A.J. Larkin, C.E. Banks, Bloodstain pattern analysis: looking at impacting blood from a different angle, *Aust. J. Forensic Sci.* 45 (2013) 85–102, doi:<http://dx.doi.org/10.1080/00450618.2012.721134>.
- [7] L. Hulse-Smith, M. Illes, A blind trial evaluation of a crime scene methodology for deducing impact velocity and droplet size from circular bloodstains, *J. Forensic Sci.* (2007) 65–69, doi:<http://dx.doi.org/10.1111/j.1556-4029.2006.00298.x>.
- [8] L. Hulse-Smith, N.Z. Mehdizadeh, S. Chandra, Deducing drop size and impact velocity from circular bloodstains, *J. Forensic Sci.* 50 (2005) 54–63, doi:<http://dx.doi.org/10.1520/JFS2003224>.
- [9] C. Knock, M. Davison, Predicting the position of the source of blood stains for angled impacts, *J. Forensic Sci.* 52 (2007) 1044–1049, doi:<http://dx.doi.org/10.1111/j.1556-4029.2007.00505.x>.
- [10] A. Patnaik, R.S. Rengasamy, V.K. Kothari, A. Ghosh, Wetting and wicking in fibrous materials, *Text. Prog.* 1 (2006) 1–105, doi:<http://dx.doi.org/10.1533/tpcr.2006.0001>.
- [11] E. Kiss, Wetting and wicking, *Text. Res. J.* 66 (1996) 660–668, doi:<http://dx.doi.org/10.1177/004051759606601008>.
- [12] T.C. de Castro, M.C. Taylor, J.A. Kieser, D.J. Carr, W. Duncan, Systematic investigation of drip stains on apparel fabrics: the effects of prior-laundering, fibre content and fabric structure on final stain appearance, *Forensic Sci. Int.* 250 (2015) 98–109, doi:<http://dx.doi.org/10.1016/j.forsciint.2015.03.004>.
- [13] T.C. De Castro, D.J. Carr, M.C. Taylor, J.A. Kieser, W. Duncan, Drip bloodstain appearance on inclined apparel fabrics: effect of prior-laundering, fibre content and fabric structure, *Forensic Sci. Int.* 266 (2016) 488–501, doi:<http://dx.doi.org/10.1016/j.forsciint.2016.07.008>.
- [14] X. Li, J. Li, S. Michielsen, Effect of yarn structure on wicking and its impact on bloodstain pattern analysis (BPA) on woven cotton fabrics, *Forensic Sci. Int.* 276 (2017) 41–50, doi:<http://dx.doi.org/10.1016/j.forsciint.2017.04.011>.
- [15] L. Dicken, C. Knock, S. Beckett, T.C. de Castro, T. Nickson, D.J. Carr, The use of micro computed tomography to ascertain the morphology of bloodstains on fabric, *Forensic Sci. Int.* 257 (2015) 369–375, doi:<http://dx.doi.org/10.1016/j.forsciint.2015.10.006>.
- [16] B. Karger, S.P. Rand, B. Brinkmann, Experimental bloodstains on fabric from contact and from droplets, *Int. J. Leg. Med.* 111 (1998) 17–21, doi:<http://dx.doi.org/10.1007/s004140050104>.
- [17] Y. Cho, F. Springer, F.A. Tulleners, W.D. Ristenpart, Quantitative bloodstain analysis: differentiation of contact transfer patterns versus spatter patterns on fabric via microscopic inspection, *Forensic Sci. Int.* 249 (2015) 233–240, doi:<http://dx.doi.org/10.1016/j.forsciint.2015.01.021>.
- [18] M. Holbrook, Evaluation of blood deposition on fabric: distinguishing spatter and transfer stains, *Int. Assoc. Bloodstain Pattern Anal. News* 26 (2010) 3–12.
- [19] J. Slemko, Bloodstains on fabric – the effects of droplet velocity and fabric, *Int. Assoc. Bloodstain Pattern Anal. News* 19 (2003) 3–11.
- [20] E.M.P. Williams, M. Dodds, M.C. Taylor, J. Li, S. Michielsen, Impact dynamics of porcine drip bloodstains on fabrics, *Forensic Sci. Int.* 262 (2016) 66–72, doi:<http://dx.doi.org/10.1016/j.forsciint.2016.02.037>.
- [21] H.F. Miles, R.M. Morgan, J.E. Millington, The influence of fabric surface characteristics on satellite bloodstain morphology, *Sci. Justice* 54 (2014) 262–266, doi:<http://dx.doi.org/10.1016/j.scijus.2014.04.002>.
- [22] British Standards Institution, *Textiles – Domestic Washing and Drying Procedures for Textile Testing BS EN ISO 6330*, (2012) .
- [23] British Standards Institution, *Textiles – Standard Atmospheres for Conditioning and Testing BS EN ISO 139*, (2005) .
- [24] British Standards Institution, *Textiles – Determination of Thickness of Textiles and Textile Products BS EN ISO 5084*, (1997) .
- [25] British Standards Institution, *Textiles – Woven Fabrics – Determination of Mass Per Unit Length and Mass Per Unit Area BS 2471*, (2005) .
- [26] British Standards Institution, *Textiles – Woven Fabrics – Construction – Methods of Analysis Part 2: Determination of the Number of Threads Per Unit Length BS EN 1049-2*, (1994) .
- [27] L. Dicken, C. Knock, D.J. Carr and S. Beckett, Investigating bloodstain dynamics at impact on the technical rear of fabric. Accepted for publication in *Forensic Sci. Int.*
- [28] J. Wu, S. Michielsen, R. Baby, Impact spatter bloodstain patterns on textiles, *J. Forensic Sci.* (2018), doi:<http://dx.doi.org/10.1111/1556-4029.13951>.
- [29] D. Brutin, B. Sobac, B. Loquet, J. Sampol, Pattern formation in drying drops of blood, *J. Fluid Mech.* 667 (2011) 85–95, doi:<http://dx.doi.org/10.1017/S0022112010005070>.
- [30] B.A.J. Larkin, C.E. Banks, Exploring the effect of specific packed cell volume upon bloodstain pattern analysis: blood drying and dry volume estimation, *J. Can. Soc. Forensic Sci.* 48 (2015) 167–189, doi:<http://dx.doi.org/10.1080/00085030.2015.1083161>.
- [31] R.D. Deegan, O. Bakajin, T.F. Dupont, G. Huber, S.R. Nagel, T.A. Witten, Capillary flow as the cause of ring stains from dried liquid drops, *Nature* 389 (1997) 827–829, doi:<http://dx.doi.org/10.1038/39827>.
- [32] A.B. Nyoni, D. Brook, Wicking mechanisms in yarns – the key to fabric wicking performance, *J. Text. Inst.* 97 (2006) 119–128, doi:<http://dx.doi.org/10.1533/joti.2005.0128>.
- [33] Metris, CT Pro User Manual, (2008) .
- [34] Volume Graphics, VGStudio Max 3.0, (2014) .